

**Anisotropic exchange coupling and stress-induced uniaxial magnetic anisotropy in Fe/GaAs(001)**Y. Fan,<sup>1</sup> H. B. Zhao,<sup>1,3</sup> G. Lüpke,<sup>1,\*</sup> A. T. Hanbicki,<sup>2</sup> C. H. Li,<sup>2</sup> and B. T. Jonker<sup>2</sup><sup>1</sup>*Department of Applied Science, College of William and Mary, Williamsburg, Virginia 23187, USA*<sup>2</sup>*Materials Science and Technology Division, Naval Research Laboratory, Washington, D.C. 20375, USA*<sup>3</sup>*Department of Optical Science and Engineering, Fudan University, Shanghai, 200433, China*

(Received 1 December 2011; published 18 April 2012)

The magnetization reversal process within the first two iron layers at the Fe/GaAs(001) interface is found to be different and independent from the Fe thin film bulk as measured by magnetic second-harmonic generation and magneto-optical Kerr effect. The interface magnetization is largely noncollinear from the bulk with an abrupt magnetic boundary and an anisotropic exchange coupling stiffness, weak interlayer coupling but relatively strong intralayer stiffness. In contrast, Fe/GaAs(110) exhibits a rigid coupling between interface and bulk magnetization suggesting that the interfacial bonding structure can dramatically change the nature of the exchange coupling. Moreover, the uniaxial magnetic anisotropy in Fe/GaAs(001) extends from the interface to the first 5 nm in the Fe film and is induced by stress. These results are also relevant to other magnetic/nonmagnetic interfaces with abrupt chemical bond structures.

DOI: [10.1103/PhysRevB.85.165311](https://doi.org/10.1103/PhysRevB.85.165311)

PACS number(s): 75.70.Cn, 75.30.Gw, 42.65.Ky

**I. INTRODUCTION**

A fundamental understanding of ferromagnetism at hetero-interfaces is crucial for the application of spintronic devices which rely on interface magnetic properties.<sup>1–5</sup> New magnetic phenomena and properties different from the bulk occur at interfaces, where an abrupt change of the bond structure induces a different electronic structure. The anisotropic electron distribution at the interface changes the ferromagnetic exchange coupling from isotropic to anisotropic.<sup>6</sup> Moreover, electron spin-orbit coupling<sup>7</sup> and strain are different at the interface, which can result in a large perpendicular magnetic anisotropy<sup>8</sup> and an in-plane uniaxial magnetic anisotropy (UMA).<sup>8–10</sup> This may cause noncollinear alignment between interface magnetization ( $M_I$ ) and bulk magnetization ( $M_B$ ).<sup>11–15</sup> The reversal behavior of  $M_I$  can also be distinctly different from  $M_B$ .<sup>11,12</sup>

The Fe/GaAs(001) interface exhibits a magnetization reversal characteristic very different from the bulk Fe layer, one-step vs two-step switching, respectively.<sup>11</sup> An in-plane UMA component dominates at the interface with easy axis along [110] direction, while in the bulk Fe film a cubic magnetic anisotropy (CMA) is prevalent with easy axes along [100] and [010] directions. The CMA to UMA ratio,  $r$ , determines the characteristics of the magnetization reversal process: one-step switching for  $r \leq 1$  and two-step switching for  $r > 1$ .<sup>16,17</sup> A large deviation angle of 40–85° was determined between  $M_I$  and  $M_B$ , and a weak interlayer exchange coupling was proposed.<sup>11</sup> However, it has not been shown whether  $M_I$  changes its orientation abruptly from  $M_B$  or whether it is still coupled to  $M_B$  by an interlayer domain wall changing its orientation gradually. The weak interlayer coupling was attributed to the unique Fe-As bonding structure at the Fe/GaAs(001) interface, but no further evidence was given in Ref. 11. Also, the nature and role of the UMA in the distinct reversal characteristics of  $M_I$  and  $M_B$  were not clearly established.

In this paper we provide further evidence which shows that within the first two Fe layers  $M_I$  sharply deviates from  $M_B$  due to the unique bond structure of the Fe/GaAs(001)

interface. The interlayer coupling is weak, while the intralayer exchange stiffness is comparable to the bulk. In contrast, Fe/GaAs(110) exhibits a rigid coupling between interface and bulk magnetization. Moreover, we find that the UMA extends from the interface to 5 nm in the Fe film and is induced by stress in Fe/GaAs(001).

The paper is structured as follows. In Sec. II the magnetic second-harmonic generation (MSHG) technique is applied to investigate the  $M_I$  reversal process, which is compared with the  $M_B$  reversal behavior obtained by magneto-optical Kerr effect (MOKE) measurements in 3-nm-thick and 8-nm-thick Fe layers grown on GaAs(001) and GaAs(110) substrates, respectively. The time-resolved (TR) MOKE technique is applied to measure magnetic anisotropy fields of Fe/GaAs(001) with Fe thickness range of 2.5–50 nm. In Sec. III we discuss two aspects of the interface magnetism of Fe/GaAs(001): the interface exchange coupling stiffness and the UMA at interface and in thin film. Conclusions of the paper are provided in Sec. IV.

**II. EXPERIMENTS**

Ultrathin Fe films with thicknesses of 2.5, 3, 5, 8, 10, 17, and 50 nm are deposited on GaAs(110)-(1 × 1) and As-terminated GaAs(001)-(2 × 4) substrates by molecular beam epitaxy (MBE) at a temperature of 10–15 °C with Fe(110)[001]//GaAs(110)[001] and Fe(001)[100]//GaAs(001)[100], respectively.<sup>2,9,18</sup> The 3-nm-thick and 8-nm-thick Fe films are capped with an approximately 2-nm-thick Fe oxide layer, and the other Fe films are covered with a 2-nm-thick Al protection layer.

The MSHG is a nonlinear optical technique used to directly investigate the buried interface magnetism, while the MOKE technique is sensitive to bulk-averaged magnetization behavior. Figure 1(a) presents the measurement geometries of MSHG and MOKE. A linear-polarized laser beam is incident on the sample. The polarization of the reflected light with doubled and fundamental frequency measures the behavior of  $M_I$  and  $M_B$ , respectively. The MSHG is able to

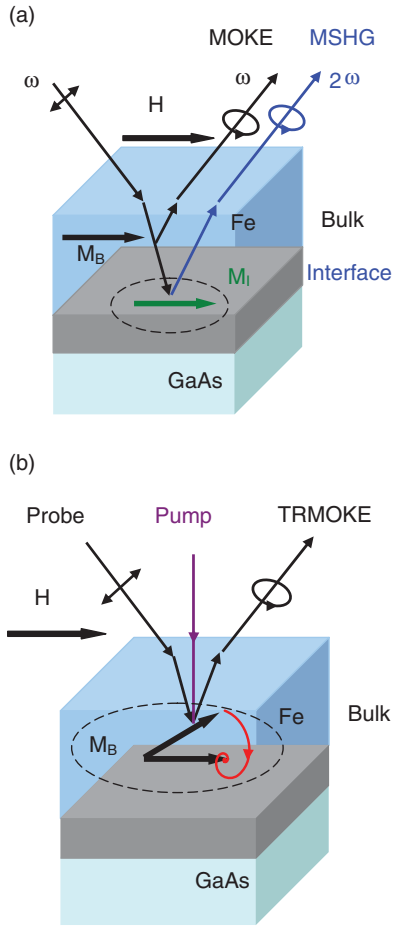


FIG. 1. (Color online) Measurement geometry of (a) MSHG and MOKE and (b) TR MOKE. (a) The interface magnetization  $M_I$  reversal process is measured by MSHG with an external magnetic field  $H$  applied along different crystal axes and is compared with the thin film bulk magnetization  $M_B$  behavior obtained by MOKE. (b) A 150-fs pulsed pump beam excites bulk magnetization precession with an applied magnetic field, which is measured using the TR MOKE technique.

selectively detect the magnetization at the interface, because it is forbidden in centro-symmetric Fe bulk and is only allowed where the inversion symmetry is broken.<sup>8,11,19</sup> To suppress MSHG from the Fe surface (where the inversion symmetry is also broken), we largely reduce the surface MSHG signal by oxidization, which greatly reduces the free electron density.<sup>20</sup> The interface magnetization induces polarization of frequency-doubled light, expressed as

$$P_i(2\omega) = \sum_{j,k} [\chi_{ijk}^-(M) E_j(\omega) E_k(\omega) + \chi_{ijk}^+(M) E_j(\omega) E_k(\omega)], \quad (1)$$

where  $P$  is the polarization,  $\chi_{ijk}$  is the susceptibility tensor component with  $\chi^\pm(-M) = \pm\chi^\pm(M)$ ,  $M$  is the magnetization, and  $E$  is the oscillating electric field of incident light.<sup>19</sup> The polarization is dependent on the magnetization due to the odd component of  $\chi$ . The  $M_I$  reversal process is measured with an external magnetic field applied along different crystal axes and is compared with the  $M_B$  behavior obtained by MOKE. For

longitudinal (MOKE) MSHG measurements a ( $p$ )  $s$ -polarized laser beam with 15- $\mu$ J pulse energy is focused on the sample with a diameter of 1.5 mm. A (photodiode) photomultiplier detects the reflected (MOKE) MSHG signal after it passes through an  $s$ -polarized analyzer and a dispersing prism. A very slow sweep rate of the magnetic field (7.47 Oe every 3 seconds) is used so that the magnetization can align along the equilibrium direction.

For quantitative characterization of the interface and bulk magnetic properties, the magnetic anisotropy fields are determined as a function of Fe layer thickness. We follow the method established by van Kampen *et al.*<sup>21</sup> to optically initiate and monitor coherent spin precession, i.e., the ferromagnetic resonance (FMR) mode, using the TR MOKE technique depicted in Fig. 1(b). We use a modulated pump beam with 30- $\mu$ J pulse energy focused to a diameter of 2 mm to induce bulk magnetization precession and detect it by a time-delayed  $p$ -polarized probe beam with 1- $\mu$ J pulse energy in a diameter of 1.5 mm. The precession of magnetization causes the polarization modulation of the reflected beam, which is measured by a photodiode after the beam passes through an  $s$ -polarized analyzer. While higher-order spin wave modes occur in the 50-nm-thick film,<sup>22</sup> uniform spin precession is observed for all Fe films.

We carry out all the measurements with a 150-fs pulsed Ti:sapphire amplifier laser system at a 1-kHz repetition rate and 800-nm wavelength. All measurements are performed at room temperature (RT).

### III. RESULTS AND DISCUSSIONS

#### A. Anisotropic interface exchange coupling stiffness

Figure 2 shows that the switching fields of interface and bulk hysteresis loops are very different for 3-nm-thick Fe layer on GaAs(001). Figures 2(a)–2(d) present  $M_I$  and  $M_B$  reversal behavior measured by longitudinal MSHG and MOKE, respectively, with the external field ( $H$ ) applied 3° away from crystallographic axis [1-10] and  $H \parallel [110]$ . The black and dark gray (red) curves are taken with  $H$  sweeping up and down, respectively. We obtain the switching field,  $H_s$ , where the two branches of the hysteresis loop separate. The crystallographic axis [1-10] is the magnetic hard axis where we observe the largest magnetization rotation before switching in Figs. 2(a) and 2(b), while the in-plane orthogonal axis [110] is the easy axis exhibiting no magnetization rotation before switching in Figs. 2(c) and 2(d). The twofold UMA dominates both at interface and in the bulk with easy axes along [110]. The results for  $H \parallel [110]$  show that  $M_I$  switches before  $M_B$  because the coercive fields are very different. Thus, the deviation angle between  $M_I$  and  $M_B$  can be as large as 180° when switching occurs at interface with  $H$  applied along the easy axis.

$M_I$  and  $M_B$  can be largely noncollinear even in the 3-nm-thick Fe layer, suggesting that there is an abrupt magnetic boundary between  $M_I$  and  $M_B$ , i.e., a sharp transition from one Fe layer to the next. If  $M_I$  were coupled to  $M_B$  by a 180° interlayer magnetic domain wall, which minimizes the sum of exchange and anisotropy energy by gradually changing orientation of  $M_I$  to  $M_B$ , the thickness of the domain wall

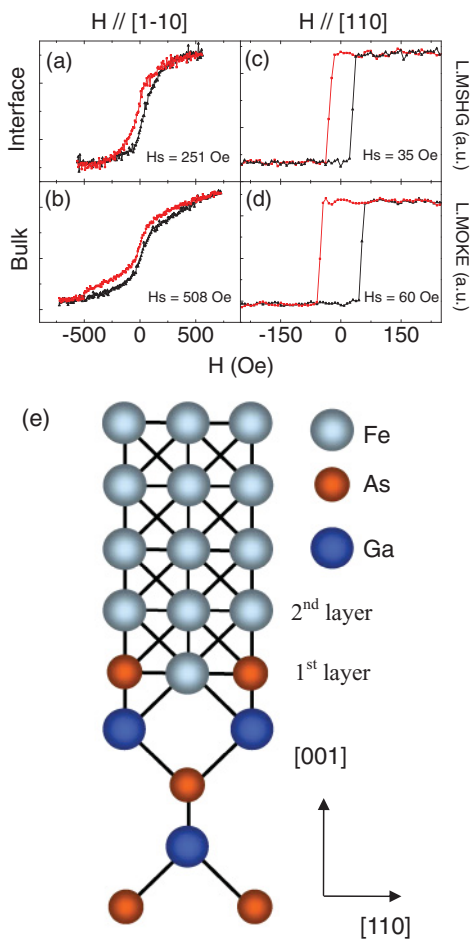


FIG. 2. (Color online) Interface and bulk magnetization reversal process and chemical bond structure for 3-nm-thick Fe film on GaAs(001). (a)–(d) Interface and bulk hysteresis loops with an external magnetic field applied  $3^\circ$  away from crystallographic axis [1-10] and along [110], measured by longitudinal MSHG and MOKE; (e) chemical bond structure of Fe/GaAs(001) from Ref. 2.

would be a few nanometers. However, such a thin domain wall would not be stable at RT. If the interlayer domain wall existed, the interlayer exchange stiffness  $A_\perp \approx (d/\pi)^2 K_u$  (Ref. 23), would be approximately  $2.2 \times 10^{-10}$  erg/cm, i.e., 4 orders of magnitude lower than in the Fe bulk, where  $d = 1$  nm (Ref. 24) is the thickness of interlayer domain wall, and  $K_u = 2.15 \times 10^5$  erg/cm<sup>3</sup> (Ref. 8) is the UMA of the interface. Thermal statistical calculation<sup>23</sup> shows that in this case the maximum ordering temperature  $T_c = 0.4$  K, where

$$T_c = A_\perp a / (0.3 K_B), \quad (2)$$

where  $a = 2.87$  Å is the Fe lattice constant, and  $K_B$  is the Boltzmann constant. Hence, no interlayer domain wall can form at RT. Therefore,  $M_I$  deviates from  $M_B$  with an abrupt magnetic boundary across which they are largely noncollinear. By using RT as the upper bound for the interlayer ordering temperature, we estimate from Eq. (2) that the interlayer exchange stiffness is *less* than  $4.3 \times 10^{-7}$  erg/cm, approximately 2/7 of the bulk value ( $1.5 \times 10^{-6}$  erg/cm).<sup>23</sup>

Next, we estimate the thickness of the magnetic interface layer. The MOKE technique averages the magnetization of the entire 3-nm-thick film, showing a signal-to-noise ratio of

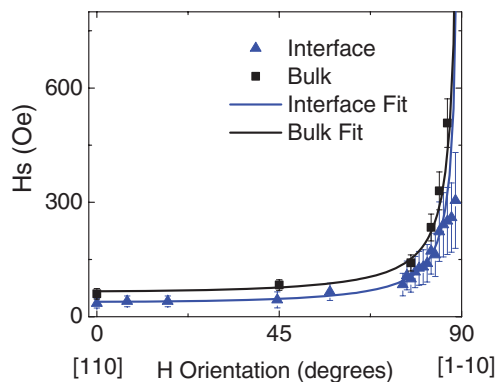


FIG. 3. (Color online) Magnitude of switching field,  $H_s$ , as a function of the magnetic field orientation with respect to the easy axis [110]. The axes of [110] and [1-10] correspond to  $0^\circ$  and  $90^\circ$  orientation in the plot.

about 15:1 [Figs. 2(b) and 2(d)]. Approximating that each iron layer contributes equally to the MOKE signal, the noise limits the thickness resolution of the MOKE measurement to 2 Å. The distinct switching of  $M_I$  is not resolved in the MOKE loop, thus we estimate the interface layer thickness to be two Fe layers. (Fe monolayer thickness is about 1.4 Å.) Figure 2(e) depicts the chemical bond structure of Fe/GaAs(001) according to Ref. 2. The GaAs(001) substrate has As dimer bonds along [1-10] and Ga dimers along [110]. During the deposition of Fe on GaAs(001)-(2 × 4), the first layer of Fe atoms occupy the vacancy sites between the GaAs lattice, and the second layer of Fe atoms displace Ga atoms to form Fe-As bonds above As atoms.<sup>2,9,25</sup> At the interface, the inversion symmetry of the first two Fe layers is broken by Fe-As bonds. Thus, MSHG probes the magnetization in the first two Fe layers, which agrees with the estimation from MOKE measurements. Both MOKE and MSHG suggest that the interface layer contains two Fe layers.

Although  $M_I$  is weakly interlayer coupled, it exhibits relatively strong intralayer coupling to support a ferromagnetic hysteresis behavior at RT. To estimate the intralayer exchange coupling stiffness, we consider the interface switching mechanism first.

A possible model to explain the switching of  $M_I$  is the magnetization rotation, which requires the magnetic field to lower the barrier of magnetic anisotropy energy to cause magnetization switching.<sup>17</sup> The switching fields are  $2(K_u/M_s + K_1/M_s) = 440$  Oe and  $2|K_u/M_s - K_1/M_s| = 248$  Oe with  $H$  applied along the hard axis [1-10] and the easy axis [110], respectively, where  $2K_u/M_s = 344$  Oe and  $2K_1/M_s = 96$  Oe are the interface in-plane UMA and CMA fields determined by TR MSHG.<sup>8</sup> The large discrepancy of switching fields between the model and the experiment (251 Oe and 35 Oe with  $H$  applied along [1-10] and [110], respectively) suggests that the magnetization rotation is not the mechanism for the observed  $M_I$  switching.

Figure 3 plots the switching field as a function of magnetic field orientation. The measured interface and thin film bulk values, represented by solid (blue) triangles and solid (black) squares, are proportional to  $1/\cos \theta$ , shown by medium gray (blue) and dark curves, where  $\theta$  is the angle between  $H$  and the easy axis [110]. This relation is consistent with the model

of pinned Neel wall displacement.<sup>23</sup> Besides, in-plane domain wall sweeping was observed in the reversal process of  $M_B$  in Fe/GaAs(001).<sup>17,26,27</sup> Since  $M_I$  and  $M_B$  exhibit similar dependence of switching field vs magnetic field orientation, both reversal processes are caused by the same mechanism, i.e., magnetic domain wall displacement triggers the reversal process of both  $M_I$  and  $M_B$ .

The switching field shows a minimum with  $H$  applied along easy axes, which is the threshold of switching field and can be expressed as<sup>23</sup>

$$H_s = \varepsilon / M_s l, \quad (3)$$

with that

$$\varepsilon = 2\sqrt{A_{//}} \int_{\pi/4}^{5\pi/4} \sqrt{(K_1/4) \sin^2 2\phi + K_u \sin^2(\phi - \pi/4)} d\phi$$

is the magnetic domain wall energy where  $A_{//}$  is the *intralayer* exchange coupling stiffness;  $K_1$  and  $K_u$  are the CMA and UMA energy, respectively;  $\phi$  is the angle between the axis [100] and the direction of in-plane magnetization;  $M_s$  is the saturated magnetization; and  $l$  is the distance between two pinning spots preventing the domain wall from moving freely. Assuming that the interface and thin film bulk contain the same pinning length and saturated magnetization, we obtain  $(\varepsilon/H_s)_{\text{interface}} = (\varepsilon/H_s)_{\text{bulk}}$  by applying Eq. (3), because they share the same switching mechanism. Using this expression, we estimate the interface intralayer exchange stiffness<sup>28</sup>  $A_{//}$  to be  $7.2 \times 10^{-7}$  erg/cm, approximately 1/2 of the bulk exchange stiffness. This results in a Curie temperature  $T_c = 502$  K for  $M_I$  using Eq. (2) and replacing  $A_{\perp}$  with  $A_{//}$ . Therefore, the estimated in-plane exchange stiffness can support a robust ferromagnetic alignment of interface spins at RT, which is consistent with the observed interface ferromagnetic behavior shown in Figs. 2(a) and 2(c). The distance between pinning spots,  $l$ , is  $0.39 \mu\text{m}$  by applying either interface or thin film bulk values to Eq. (3).

The Fe interface layer exhibits anisotropic exchange strength and weak *interlayer* but relatively strong intralayer coupling. Skomski *et al.*<sup>6</sup> attributed this effect to an anisotropic distribution of electrons induced by bond formation at the interface and suggested that the exchange stiffness,  $A$ , needs to be represented by a  $3 \times 3$  tensor. The As  $p$ -Fe  $d$  hybridization causes the anisotropy in the density of states of  $3d$  electrons near the Fermi energy. This could induce more electronic states within the interface layer, which causes the stronger intralayer coupling. However, the overall correlation effect of  $3d$  electrons is reduced due to  $3d$  band broadening, which reduces both the inter- and intralayer exchange strength at the interface. The quantitative analysis of the interface exchange tensor requires a detailed first-principle investigation of the spin-dependent density of states, which is beyond the scope of this paper.

To corroborate that the interface chemical bonding structure greatly affects the interlayer exchange coupling, we conducted comparison measurements on the 8-nm-thick Fe layer on GaAs(110).

We observe similar switching processes for  $M_I$  and  $M_B$ , and the interface and bulk magnetizations have nearly the same switching fields, as shown in Figs. 4(a)–4(d). This indicates that  $M_I$  and  $M_B$  are rigidly coupled. Previous studies showed

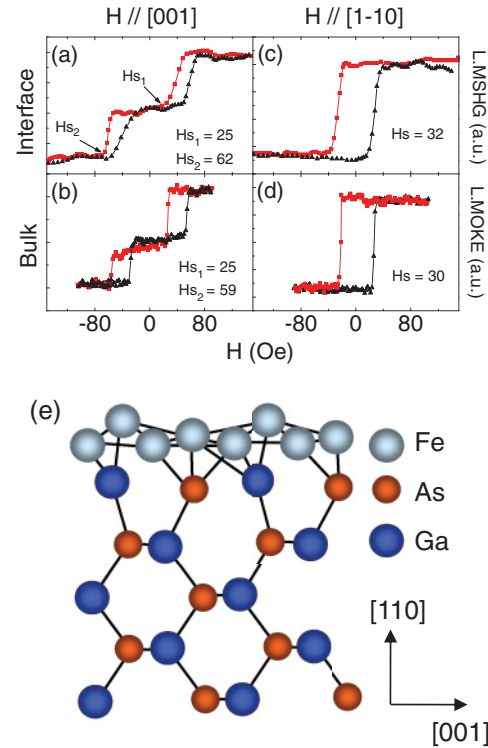


FIG. 4. (Color online) Interface and bulk magnetization reversal process and chemical bond structure for 8-nm-thick Fe film on GaAs(110). (a)–(d) Interface and bulk hysteresis loops with an external magnetic field applied along [001] and [1-10], measured by longitudinal MSHG and MOKE; (e) chemical bond structure of Fe/GaAs(110) from Ref. 31.

that Fe/GaAs(110) exhibits twofold UMA with easy axes along [1-10] and [-110] and fourfold CMA with easy axes along [001], [1-10], [00-1], and [-110].<sup>29,30</sup> In our sample the crystallographic axis [1-10] is the magnetic easy axis, and we observe no magnetization rotation before single-step switching, as shown in Figs. 4(c) and 4(d). The [001] axis is the intermediate easy axis, where a kink is revealed in the hysteresis loop in Figs. 4(a) and 4(b). Such a kink arises from a two-jump process, with the first jump of the magnetization from a local minimum of free energy [001] to a global minimum [1-10] and the second jump from [1-10] to [00-1].

The difference in the interlayer magnetization coupling for the two interfaces of Fe/GaAs with different crystal planes, (110) vs (001), implies that interface bonds can dramatically affect the interlayer exchange coupling strength. Figure 4(e) shows the calculated atomic structure of Fe/GaAs(110) with lowest energy following Ref. 31. The surface of GaAs(110) substrate contains both As and Ga atoms, which form “zig-zag ridges” parallel to [1-10].<sup>18</sup> Unlike Fe/GaAs(001) interface where all interface Fe atoms bond with As [Fig. 2(e)], there are Fe atoms bonding only with Ga at the Fe/GaAs(110) interface. The Ga-Fe bond is weak and so is the  $p$ - $d$  hybridization.<sup>31</sup> It has little effect on the  $3d$  band and the anisotropy of electron distribution, resulting in a bulklike exchange property at interface. Besides, the interface lattice positions of Fe atoms and the direction of Fe-As bonds are different between Fe/GaAs(110) and (001). All these bonding differences induce



distinct electronic structures at the two interfaces, causing different strengths and anisotropies of the interface exchange coupling.

### B. Stress-induced UMA

Finally, we investigate the evolution of the magnetic anisotropy, especially the UMA component, from interface to bulk in Fe/GaAs(001).

Figure 5(a) shows coherent spin precession in 2.5-nm-thick Fe film on GaAs(001) measured by TR MOKE. The background signal due to heat diffusion has been subtracted from the data. The precession can be fitted by a damped sine wave. The Fourier spectrum [Fig. 5(a) inset] exhibits a uniform mode of spin precession. The effective UMA and CMA fields are determined by fitting the angular frequency of uniform precession vs magnetic field data to the following formula:

$$\omega = \gamma[(H \cos(\delta - \phi) + H^\alpha)(H \cos(\delta - \phi) + H^\beta)]^{1/2}, \quad (4)$$

derived from the Landau-Lifshitz-Gilbert (LLG) equation, with

$$H^\alpha = 2K_1 \cos(4\phi)/M_s + 2K_u \sin(2\phi)/M_s,$$

$$H^\beta = 4\pi M_s + 2K_\perp/M_s + K_1[2 - \sin^2(2\phi)]/M_s - K_u(\sin \phi - \cos \phi)^2/M_s,$$

and  $\gamma = \gamma_e g/2$  (for Fe,  $g = 2.09$  and  $\gamma_e = 1.76 \times 10^7$  Hz/Oe) is the gyromagnetic ratio. The angles  $\phi$  and  $\delta$  are angles with respect to the axis [100] for the directions of in-plane magnetization and applied magnetic field  $H$ , respectively.  $K_u$ ,  $K_1$ , and  $K_\perp$  are in-plane UMA, CMA, and out-of-plane anisotropy energy, respectively.<sup>32</sup> Figure 5(b) shows the field dependence of precession frequency and the corresponding fits to Eq. (4) with  $H$  parallel with [1-10] direction. The model describes the data very well.

Figure 5(c) shows the UMA and CMA field ( $2K_u/M_s$  and  $2K_1/M_s$ , respectively) as a function of Fe film thickness. The solid square (blue) and triangle (black) symbols represent the bulk values, and the open square (blue) and triangle (black) symbols plot the interface anisotropy fields from the 8-nm-thick Fe film grown on GaAs(001), as determined by TR MSHG in Ref. 8. The curves (blue and black) are guides to the eye. The UMA field is almost constant within the first 5 nm, although a difference of  $44 \pm 28$  Oe is observed between 2.5 and 5 nm, but undergoes a rapid decrease between 5 and 10 nm thickness. Its value can be neglected as the thickness increases to 50 nm. This result indicates that the UMA field is extended from the interface to 5 nm in the Fe film on the As-terminated GaAs(001)-(2 × 4) substrate. The evolution of UMA qualitatively agrees with the reported study on the Ga-terminated GaAs(001)-(4 × 6) substrate, showing dominant UMA field in the 1-nm-thick Fe film.<sup>10</sup> The different substrate reconstruction could affect the extension depth of UMA. In contrast, the CMA field increases with thickness due to increasing spin-orbit coupling in the Fe thin film.

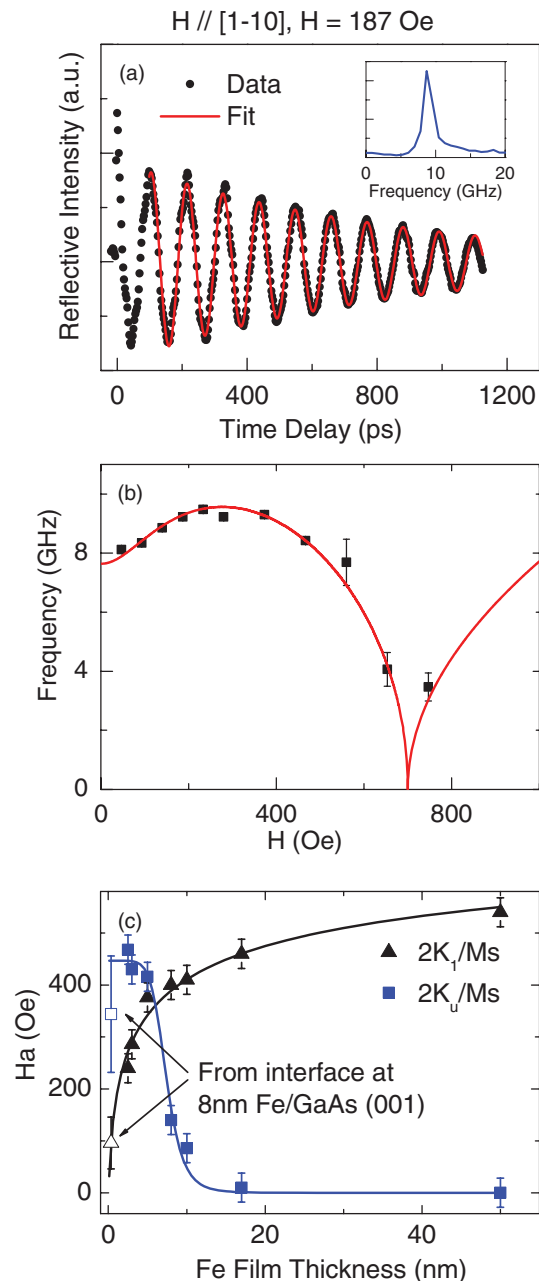


FIG. 5. (Color online) TR MOKE measurements and thickness dependence of magnetic anisotropy fields for Fe/GaAs(001). (a) Coherent spin precession in 2.5-nm-thick Fe film on GaAs(001) measured by TR MOKE with  $H = 187$  Oe applied along the crystallographic axis [1-10]. The data, black dots, are fitted by a damped sine wave, dark gray (red) curve. The Fourier spectrum in the inset indicates a uniform mode of Fe spin precession. (b) Spin precession frequency as a function of magnetic field for the same sample and geometry as in (a). The dark gray (red) curve is a fit of Eq. (4). (c) Magnetic anisotropy fields as a function of Fe film thickness in Fe/GaAs(001) measured by TR MOKE. Uniaxial and cubic magnetic anisotropy fields of bulk layer are represented by solid squares (blue) and solid triangles (black), respectively. The values of 8-nm-thick and 50-nm-thick Fe films are taken from Refs. 8 and 22, respectively. The open square (blue) and open triangle (black) symbols represent the corresponding interface anisotropy fields determined from the 8-nm-thick Fe film in Ref. 8. The curves (blue and black) are guides to the eye.

We find that the thickness dependence of UMA is closely related to the Fe island formation during growth of the first 5-nm-thick Fe layer and starts to disappear beyond.<sup>33</sup> The Fe-As bond induces a tensile stress, instead of compressive stress arising from lattice mismatch and substrate-dependent tetragonal distortion at Fe/GaAs interface,<sup>34</sup> which is dominant in the film thickness range of 2–6 nm, due to some As atoms' diffusion into Fe.<sup>35</sup> The interface island elongation along [1-10] is caused by the preference of Fe growing along the direction of the As dimer bond.<sup>33</sup> This suggests that the tensile stress,  $\sigma$ , is uniaxial and collinear to [1-10] ( $\sigma_{[1-10]} > 0$ ). The product of  $\sigma_{[1-10]}\lambda_{[1-10]} < 0$  indicates that the axis [1-10] is the uniaxial hard axis, consistent with the experimental observation, where  $\lambda_{[1-10]} < 0$  is the Fe magnetostrictive coefficient along [1-10].<sup>36</sup>

The UMA field evolution in the Fe thin film can be expressed as  $K_u = \kappa/t - 3(\sigma\lambda)_{[1-10]}/2$ , where  $\kappa$  is the uniaxial crystalline anisotropy,  $t$  is the film thickness, and  $\sigma$  is the stress of the entire film. Our results do not show a linear dependence between the measured UMA and reciprocal film thickness. So  $\kappa$  is not the main contribution, and UMA does not directly arise from a new type of spin-orbital coupling induced by Fe-As bonds. Actually, the statement that UMA is directly induced by Fe-As bonds was challenged by the observation that some cap layers erase the dominant UMA in ultrathin Fe layer on GaAs(001) and was discussed by several groups.<sup>37,38</sup> Our result shows that UMA is mainly a stress-induced magnetoelastic anisotropy, and its thickness dependence is controlled by stress within Fe islands during film growth. Within the first 5 nm of thickness, islands with tensile stress form, and UMA dominates both at interface and bulk layer. However, beyond 5 nm, the tensile stress relaxes<sup>35</sup> with the merging of islands. Moreover, the relaxed stress could further reduce the magnetostrictive coefficient.<sup>39,40</sup>

Thus UMA decreases rapidly in the Fe film and CMA dominates.

#### IV. CONCLUSIONS

In conclusion, the interface magnetization reversal process in Fe/GaAs(001) is found to be different and quite independent from the Fe bulk layer even at small 3-nm film thickness. Our analysis shows that the magnetization within the first two Fe layers at the interface is largely noncollinear from the bulk layer with an abrupt magnetic boundary. The interface magnetization of Fe/GaAs(001) exhibits an anisotropic exchange coupling stiffness which is weak interlayer coupling (less than 2/7 of the bulk value) but relatively strong intralayer stiffness (approximately 1/2 of the bulk value), while Fe/GaAs(110) reveals a rigid coupling between interface and bulk layer. This result indicates that chemical bond structure can dramatically change the nature of interface exchange coupling. Although interface magnetization is weakly coupled with bulk in Fe/GaAs(001), UMA is extended from interface to bulk within the first 5 nm and is induced by stress.

The anisotropic exchange coupling and the distinct magnetic anisotropy are certainly not limited to the Fe/GaAs(001) interface. These interface-induced magnetic properties can exist at other ferromagnetic/nonmagnetic interfaces at which the elemental constituents form abrupt chemical bond structures.

#### ACKNOWLEDGMENTS

The work at the College of William and Mary was supported by the Office of Naval Research. The work at Naval Research Laboratory was supported by core programs. The work at Fudan University was supported by National Natural Science Foundation of China (60908005) and Shanghai Pujiang program.

\*Corresponding author: gxluep@wm.edu

<sup>1</sup>B. T. Jonker, in *Ultrathin Magnetic Structures IV*, edited by B. Heinrich and J. A. C. Bland (Springer, New York, 2005), p. 19.

<sup>2</sup>T. J. Zega, A. T. Hanbicki, S. C. Erwin, I. Zutic, G. Kioseoglou, C. H. Li, B. T. Jonker, and R. M. Stroud, *Phys. Rev. Lett.* **96**, 196101 (2006).

<sup>3</sup>W. Hubner and K. H. Bennemann, *Phys. Rev. B* **40**, 5973 (1989).

<sup>4</sup>E. I. Rashba, *Phys. Rev. B* **62**, R16267 (2000).

<sup>5</sup>T. L. Monchesky, A. Enders, R. Urban, K. Myrtle, B. Heinrich, X.-G. Zhang, W. H. Butler, and J. Kirschner, *Phys. Rev. B* **71**, 214440 (2005).

<sup>6</sup>R. Skomski, A. Kashyap, J. Zhou, and D. J. Sellmyer, *J. Appl. Phys.* **97**, 10B302 (2005).

<sup>7</sup>J. S. Claydon, Y. B. Xu, M. Tselepi, J. A. C. Bland, and G. van der Laan, *Phys. Rev. Lett.* **93**, 037206 (2004).

<sup>8</sup>H. B. Zhao, D. Talbayev, G. Lüpke, A. T. Hanbicki, C. H. Li, and B. T. Jonker, *Appl. Phys. Lett.* **91**, 052111 (2007).

<sup>9</sup>E. M. Kneidler, B. T. Jonker, P. M. Thibado, R. J. Wagner, B. V. Shanabrook, and L. J. Whitman, *Phys. Rev. B* **56**, 8163 (1997).

<sup>10</sup>Kh. Zakeri, Th. Kebe, J. Lindner, and M. Farle, *J. Mag. Mag. Mater.* **299**, L1 (2006).

<sup>11</sup>H. B. Zhao, D. Talbayev, G. Lüpke, A. T. Hanbicki, C. H. Li, M. J. van't Erve, G. Kioseoglou, and B. T. Jonker, *Phys. Rev. Lett.* **95**, 137202 (2005).

<sup>12</sup>Y. Fan, K. J. Smith, G. Lüpke, A. T. Hanbicki, C. H. Li, H. B. Zhao, and B. T. Jonker, Exchange bias of the interface spin system at the ferromagnet/oxide interface, submitted to *Nat. Nano.* (2011) (unpublished).

<sup>13</sup>M. Gruyters, T. Bernhard, and H. Winter, *Phys. Rev. Lett.* **94**, 227205 (2005).

<sup>14</sup>F. Sirotti, S. Giraldo, P. Prieto, L. Floreano, G. Panaccione, and G. Rossi, *Phys. Rev. B* **61**, R9221 (2000).

<sup>15</sup>R. Allenspach, M. Taborelli, M. Landolt, and H. C. Siegmann, *Phys. Rev. Lett.* **56**, 953 (1986).

<sup>16</sup>C. Daboo, R. J. Hicken, D. E. P. Eley, M. Gester, S. J. Gray, A. J. R. Ives, and J. A. C. Bland, *J. Appl. Phys.* **75**, 5586 (1994).

<sup>17</sup>C. Daboo, R. J. Hicken, E. Gu, M. Gester, S. J. Gray, D. E. P. Eley, E. Ahmad, J. A. C. Bland, R. Ploessl, and J. N. Chapman, *Phys. Rev. B* **51**, 15964 (1995).

<sup>18</sup>G. A. Prinz and J. J. Krebs, *Appl. Phys. Lett.* **39**, 397 (1981).

<sup>19</sup>R.-P. Pan, H. D. Wei, and Y. R. Shen, *Phys. Rev. B* **39**, 1229 (1989).

- <sup>20</sup>J. Reif, J. C. Zink, C.-M. Schneider, and J. Kirschner, *Phys. Rev. Lett.* **67**, 2878 (1991).
- <sup>21</sup>M. van Kampen, C. Jozsa, J. T. Kohlhepp, P. LeClair, L. Lagae, W. J. M. de Jonge, and B. Koopmans, *Phys. Rev. Lett.* **88**, 227201 (2002).
- <sup>22</sup>H. B. Zhao, D. Talbayev, Y. Fan, G. Lüpke, A. T. Hanbicki, C. H. Li, and B. T. Jonker, *Phys. Stat. Sol. (c)* **5**, 2627 (2008).
- <sup>23</sup>S. Chikazumi, in *Physics of Ferromagnetism*, 2nd ed., edited by J. Birman, S. F. Edwards, R. Friend, C. H. Llewellyn Smith, M. Rees, D. Sherrington, and G. Veneziano (Oxford, New York, 1997), Chap. 16, Spin distribution and domain walls; Chap. 18, Technical magnetization, p. 407–517.
- <sup>24</sup>We choose  $d = 1$  nm just for simplicity. Increasing  $d$  by a factor of 3 only increases the critical temperature  $T_c$  by a factor of 1.27, which is still well below room temperature.
- <sup>25</sup>S. C. Erwin, S.-H. Lee, and M. Scheffler, *Phys. Rev. B* **65**, 205422 (2002).
- <sup>26</sup>E. Gu, J. A. C. Bland, C. Daboo, M. Gester, L. M. Brown, R. Ploessl, and J. N. Chapman, *Phys. Rev. B* **51**, 3596 (1995).
- <sup>27</sup>W. Y. Lee, B.-Ch. Choi, Y. B. Xu, and J. A. C. Bland, *Phys. Rev. B* **60**, 10216 (1999).
- <sup>28</sup>To estimate  $A_{//}$  at interface, we use  $K_u = 2.15 \times 10^5$  erg/cm<sup>3</sup> and  $K_1 = 6.0 \times 10^4$  erg/cm<sup>3</sup> from Ref. 8;  $H_s = 35$  Oe, thin film bulk values of  $A_{//} = 1.5 \times 10^{-6}$  erg/cm,  $K_u = 2.69 \times 10^5$  erg/cm<sup>3</sup>,  $K_1 = 1.79 \times 10^5$  erg/cm<sup>3</sup>,  $H_s = 60$  Oe determined from 3-nm-thick Fe film, and  $M_s = 1.25 \times 10^3$  emu/cm<sup>3</sup> measured for thin Fe film in Ref. 7.
- <sup>29</sup>M. Gester, C. Daboo, R. J. Hicken, S. J. Gray, A. Ercole, and J. A. C. Bland, *J. Appl. Phys.* **80**, 347 (1996).
- <sup>30</sup>G. A. Prinz, G. T. Rado, and J. J. Krebs, *J. Appl. Phys.* **53**, 2087 (1982).
- <sup>31</sup>A. Grünebohm, H. C. Herper, and P. Entel, *Phys. Rev. B* **80**, 064417 (2009).
- <sup>32</sup>H. B. Zhao, D. Talbayev, Q. G. Yang, G. Lüpke, A. T. Hanbicki, C. H. Li, O. M. J. van't Erve, G. Kioseoglou, and B. T. Jonker, *Appl. Phys. Lett.* **86**, 152512 (2005).
- <sup>33</sup>P. M. Thibado, E. Kneedler, B. T. Jonker, B. R. Bennett, B. V. Shanabrook, and L. J. Whitman, *Phys. Rev. B* **53**, R10481 (1996).
- <sup>34</sup>R. A. Gordon, E. D. Crozier, D.-T. Jiang, T. L. Monchesky, and B. Heinrich, *Phys. Rev. B* **62**, 2151 (2000).
- <sup>35</sup>G. Wedler, B. Wassermann, R. Nötzel, and R. Koch, *Appl. Phys. Lett.* **78**, 1270 (2001).
- <sup>36</sup>R. C. O'Handley, *Modern Magnetic Materials: Principles and Applications* (Wiley, New York, 2000), p. 221.
- <sup>37</sup>M. Madami, S. Tacchi, G. Carlotti, G. Gubbiotti, and R. L. Stamps, *Phys. Rev. B* **69**, 144408 (2004).
- <sup>38</sup>B. Aktaş, B. Heinrich, G. Woltersdorf, R. Urban, L. R. Tagirov, F. Yıldız, K. Özdoğan, M. Özdemir, O. Yalçın, and B. Z. Rameev, *J. Appl. Phys.* **102**, 013912 (2007).
- <sup>39</sup>A. Enders, D. Sander, and J. Kirschner, *J. Appl. Phys.* **85**, 5279 (1999).
- <sup>40</sup>R. Koch, M. Weber, K. Thirmer, and K. H. Rieder, *J. Magn. Magn. Mater.* **159**, L11 (1996).